BRAIN COMMUNICATIONS

# Hindlimb motor responses to unilateral brain injury: spinal cord encoding and left-right asymmetry

Mengliang Zhang,[1,2,†] Hiroyuki Watanabe,[3,†] Daniil Sarkisyan,[3] Marlene Storm Andersen,[2] Olga Nosova,[3] Vladimir Galatenko,[4,*] Liliana Carvalho,[5] Nikolay Lukoyanov,[5] Jonas Thelin,[1] Jens Schouenborg[1,‡] and Georgy Bakalkin[3,‡]

*Present address: Evotec International GmbH, Göttingen, Germany.

†These authors contributed equally to this work.

‡These authors are co-senior authors.

Mechanisms of motor deficits (e.g. hemiparesis and hemiplegia) secondary to stroke and traumatic brain injury remain poorly understood. In early animal studies, a unilateral lesion to the cerebellum produced postural asymmetry with ipsilateral hindlimb flexion that was retained after complete spinal cord transection. Here we demonstrate that hindlimb postural asymmetry in rats is induced by a unilateral injury of the hindlimb sensorimotor cortex, and characterize this phenomenon as a model of spinal neuroplasticity underlying asymmetric motor deficits. After cortical lesion, the asymmetry was developed due to the contralesional hindlimb flexion and persisted after decerebration and complete spinal cord transection. The asymmetry induced by the left-side brain injury was eliminated by bilateral lumbar dorsal rhizotomy, but surprisingly, the asymmetry after the right-side brain lesion was resistant to deafferentation. Pancuronium, a curare-mimetic muscle relaxant, abolished the asymmetry after the right-side lesion suggesting its dependence on the efferent drive. The contra- and ipsilesional hindlimbs displayed different musculo-articular resistance to stretch after the left but not right-side injury. The nociceptive withdrawal reflexes evoked by electrical stimulation and recorded with EMG technique were different between the left and right hindlimbs in the spinalized decerebrate rats. On this asymmetric background, a brain injury resulted in greater reflex activation on the contra- versus ipsilesional side; the difference between the limbs was higher after the right-side brain lesion. The unilateral brain injury modified expression of neuroplasticity genes analysed as readout of plastic changes, as well as robustly impaired coordination of their expression within and between the ipsi- and contralesional halves of lumbar spinal cord; the effects were more pronounced after the left side compared to the right-side injury. Our data suggest that changes in the hindlimb posture, resistance to stretch and nociceptive withdrawal reflexes are encoded by neuroplastic processes in lumbar spinal circuits induced by a unilateral brain injury. Two mechanisms, one dependent on and one independent of afferent input may mediate asymmetric hindlimb motor responses. The latter, deafferentation resistant mechanism may be based on sustained muscle contractions which often occur in patients with central lesions and which are not evoked by afferent stimulation. The unusual feature of these mechanisms is their lateralization in the spinal cord.

1 Department of Experimental Medical Science, Neuronano Research Center, Lund University, 221 00 Lund, Sweden
2 Department of Molecular Medicine, University of Southern Denmark, DK-5000 Odense, Denmark
3 Department of Pharmaceutical Biosciences, Uppsala University, 751 24 Uppsala, Sweden
4 Faculty of Mechanics and Mathematics, Lomonosov Moscow State University, 119234 Moscow, Russia
5 Departamento de Biomedicina da Faculdade de Medicina da Universidade do Porto, Instituto de Investigação e Inovação em Saúde, Instituto de Biologia Molecular e Celular, 4200-319 Porto, Portugal

Received February 8, 2020. Revised April 2, 2020. Accepted April 7, 2020. Advance Access publication April 30, 2020

Correspondence to: Georgy Bakalkin, PhD, Professor Department of Pharmaceutical Biosciences, Uppsala University, 751 24 Uppsala, Sweden
E-mail: georgy.bakalkin@farmbio.uu.se

**Keywords:** brain injury; hindlimb motor deficits; lateralization; postural asymmetry; nociceptive withdrawal reflexes

**Abbreviations:** $AI_{C/I}$ = the contra/ipsilesional asymmetry index; $AI_{L/R}$ = the Left/Right asymmetry index; $AI_{SN}$ = the asymmetry index in the spike number; $AI_{Thr}$ = the asymmetry index in stimulation threshold; EDL = extensor digitorum longus; HL-PA = hindlimb postural asymmetry; HPDCI = highest posterior density continuous intervals; Int = interrossei; MPA = magnitude of postural asymmetry; NWR = nociceptive withdrawal reflex; $P_A$ = probability to develop asymmetry; $P_C$ = probability to flex the contralesional hindlimb; PL = peroneus longus; SN = the number of spikes; TBI = traumatic brain injury; Thr = stimulation threshold; UBI = a unilateral ablation brain injury; W = work

**Graphical Abstract**

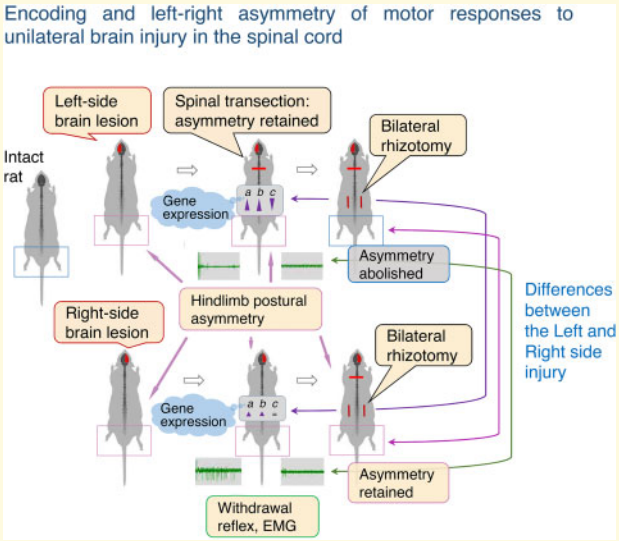


# Introduction

Traumatic brain injury (TBI) and stroke cause sensorimotor impairments including muscle weakness, spasticity, and stretch and effort-unrelated sustained muscle contractions (Gracies, 2005; Murphy and Corbett, 2009; Grau, 2014; Rousseaux *et al.*, 2014; Kerzoncuf *et al.*, 2015; Pin-Barre and Laurin, 2015; Feldman and Levin, 2016; Jones, 2017; Marinelli *et al.*, 2017; Wilson *et al.*, 2017; Lorentzen *et al.*, 2018). In patients, stroke and TBI are mostly unilateral and often result in formation of postural asymmetry with contralateral hemiplegia and hemiparesis. Clinically well-recovered stroke survivors still have a substantial postural asymmetry in the relative contribution of each leg to body sway control (Roelofs *et al.*, 2018). Plastic rearrangements in supraspinal and spinal neurocircuitries induced by aberrant asymmetric activity of descending neural tracts may underlie motor impairments or contribute to motor recovery. In contrast to adaptive changes in the brain, knowledge of brain injury-induced spinal plasticity is limited (Patterson, 2001; Tan *et al.*, 2012; Wolpaw, 2012; Sist *et al.*, 2014; Tennant, 2014; Pin-Barre and Laurin, 2015). Evidence for asymmetric 'spinal memory' was presented in early studies by DiGiorgio (1929, 1942) and other researchers (Chamberlain *et al.*, 1963; Patterson, 2001). They demonstrated that a hemicerebellar lesion causes lasting changes in spinal cord functions manifested as the ipsilesional hindlimb flexion and that the hindlimb postural asymmetry (HL-PA) is retained after complete spinal transection. Consistently, monosynaptic and polysynaptic reflexes are enhanced on the ipsilateral side after lateral hemisection of the spinal cord, and this change is sustained after complete spinal transection performed caudally to the hemisection level (Hultborn and Malmsten, 1983*a*, *b*; Malmsten, 1983; Frigon *et al.*, 2009; Rossignol and Frigon, 2011; Gossard *et al.*, 2015). The HL-PA is an attractive animal model to unravel mechanisms of pathological 'spinal memory', which may underlie asymmetric motor deficits including hemiplegia and hemiparesis.

A number of clinical studies focused on changes in monosynaptic reflexes induced by stroke or TBI whereas there is a paucity of studies that analyse polysynaptic reflexes (Delwaide and Oliver, 1988; Thilmann *et al.*, 1991; Wilson *et al.*, 1999; Aymard *et al.*, 2000; Condliffe *et al.*, 2005; Dietz *et al.*, 2009; Hubli *et al.*, 2012). The polysynaptic nociceptive withdrawal reflexes

(NWRs) may be useful tools for the investigation of pathological changes in the spinal cord, given that these changes are due to converging inputs from the peripheral afferents and descending motor commands to spinal neurons (Crenna and Frigo, 1984; Duysens *et al.*, 1990; Duysens *et al.*, 1992; Rossi and Decchi, 1994; Andersen *et al.*, 1995; Spaich *et al.*, 2004; Sandrini *et al.*, 2005; Spaich *et al.*, 2006; Emborg *et al.*, 2009). Only a few studies have investigated changes in NWR excitability in post-stroke hemiparetic patients with limb motor deficits (Spaich *et al.*, 2006; Serrao *et al.*, 2012; Rueterbories *et al.*, 2013; Spaich *et al.*, 2014). The NWR-related EMG kinematic responses were increased and NWR modulation impaired in stroke patients with hemiparesis (Serrao *et al.*, 2012; Alvisi *et al.*, 2018). The NWR-based functional electrical therapy was found to be useful in the rehabilitation of gait in severely impaired hemiparetic patients by improving post-treatment walking velocity and gait symmetry (Spaich *et al.*, 2014; Gervasio *et al.*, 2018). There is a deficit of mechanistic animal studies that analysed pathological changes in the hindlimb NWRs and their role in sensorimotor impairments induced by brain injury.

Several neurological phenomena are differently developed after injury to the left and right hemisphere. The right side compared to the left-side stroke results in poorer postural responses in quiet and perturbed balance suggesting a prominent role of the right hemisphere in efferent control of balance (Fernandes *et al.*, 2018). Hemineglect and bias of the subjective vertical are general causes of postural asymmetry and instability (Tasseel-Ponche *et al.*, 2015). The serious postural impairment—the contraversive pushing called 'Pusher syndrome', which is linked to biased verticality and hemispatial neglect, is more common among patients with the right rather than left-hemisphere lesions (Perennou *et al.*, 2008). Components in trunk control may be impaired depending on the side of the lesion. 'Postural instability' is significantly more frequent among patients with right-hemisphere lesions, while 'apraxic responses' predominate among those with left-hemisphere injury (Spinazzola *et al.*, 2003). Consistently, animal studies showed that changes in locomotor behaviour and correlated region-specific differences in turnover of neurotransmitters after somatosensory TBI were dependent on the side of brain injury (Robinson, 1979; Pearlson and Robinson, 1981; Spinazzola *et al.*, 2003; Perennou *et al.*, 2008; Sainburg, 2014; Sainburg *et al.*, 2016; Ocklenburg *et al.*, 2017; Fernandes *et al.*, 2018; Stancher *et al.*, 2018). Right but not left somatosensory lesions produced behavioural hyperactivity and bilaterally decreased cerebral and locus ceruleus norepinephrine concentrations.

In this study, the HL-PA phenomenon was characterized as a model of asymmetric hindlimb motor deficits induced by a unilateral injury of the hindlimb representation area of the sensorimotor cortex. We examined whether a unilateral ablation brain injury (UBI) induces HL-PA; whether the fore limbs are also affected; whether the contra- or ipsilesional leg is flexed; and whether HL-PA is encoded at the spinal level and persists after complete spinal cord transection. The suction lesion was performed to restrict a damaged area to the hindlimb sensorimotor cortex with the aim to examine specific changes in hindlimb motor functions and lumbar spinal circuits. Effects of the left- and right-side lesions were studied because of lateralization of the sensorimotor system and its differential responses to the left- and right-side injuries (Robinson, 1979; Pearlson and Robinson, 1981; Spinazzola *et al.*, 2003; Perennou *et al.*, 2008; Sainburg, 2014; Sainburg *et al.*, 2016; Ocklenburg *et al.*, 2017; Fernandes *et al.*, 2018; Stancher *et al.*, 2018). In parallel with the HL-PA, we evaluated whether the hindlimb NWRs are affected by the UBI. We also examined whether HL-PA formation depends on sensory feedback and spinal motor output. Expression of plastic genes was analysed as a readout of neuroplastic changes in the lumbar spinal cord induced by injury of the hindlimb sensorimotor cortex. Genes selected for analysis were transcriptional regulators of synaptic plasticity (*cFos*, *Egr1* and *Nfkbia*), regulators of axonal sprouting, synapse formation, neuronal survival and neuroinflammation (*Arc*, *Bdnf*, *Dlg4*, *Homer-1*, *Gap43*, *Syt4* and *Tgfb1*), essential components of the glutamate system critical for neuroplastic responses (*GluR1*, *Grin2a* and *Grin2b*), and all are expressed in the spinal cord.

# Materials and methods

All methods and materials are described in detail in Supplementary material section.

Adult male Sprague Dawley rats (Taconic, Denmark) weighing 170–430 g (see Supplementary Table 1) were used in the study. The animals received food and water *ad libitum*, and were kept in a 12-h day–night cycle at a constant environmental temperature of 21°C (humidity: 65%) and randomly assigned to their respective experimental groups. Approval for animal experiments was obtained from the Malmö/Lund ethics committee on animal experiments (No.: M7-16), and the ethics committee of the Faculty of Medicine of Porto University and Portuguese Direção-Geral de Alimentação e Veterinária (No. 0421/000/000/2018). All animals were analysed in a single test excluding 11 right-side sham and 14 right-side UBI rats analysed in both HL-PA and EMG experiments (Supplementary Table 1).

## Brain surgery and histology

The rats were anaesthetized with 3% isoflurane (Abbott, Norway) in a mixture with 65% nitrous oxide and 35% oxygen. The hindlimb sensorimotor cortex was removed by gentle suction through a pipette (tip diameter 0.5 mm) (Fig. 1) (for details, see 'Supplementary materials'). Control (sham) animals underwent the same procedure but cortex was not aspirated.

The localization and size of the lesion were analysed after perfusion with 4% paraformaldehyde. Following an

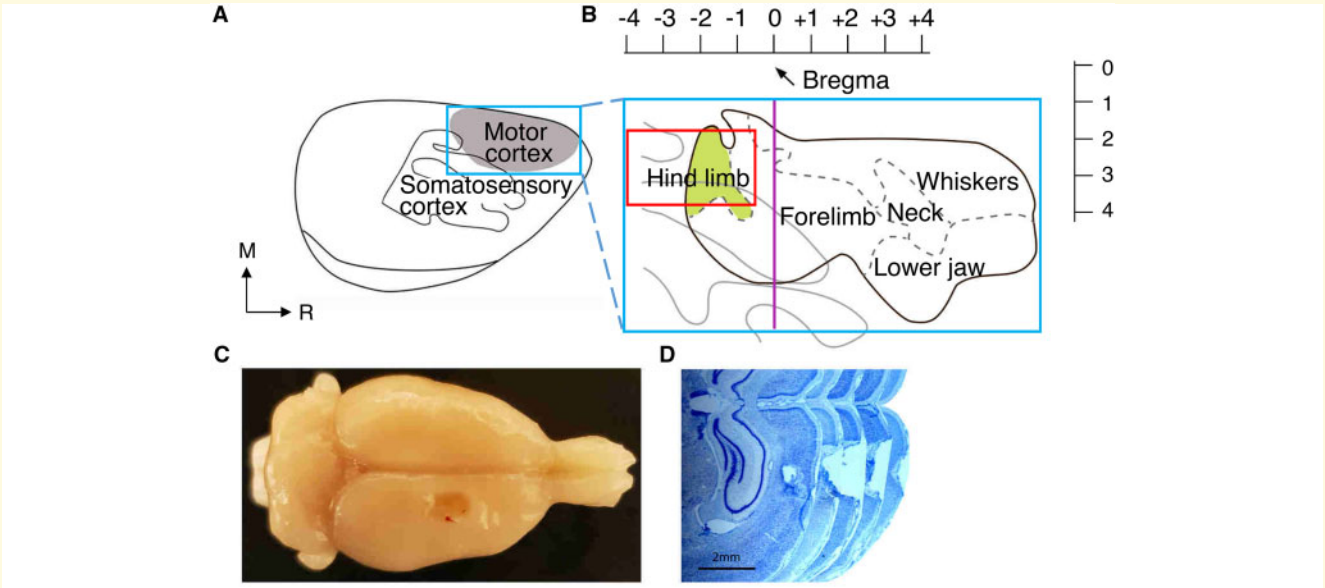


**Figure 1 An UBI of the hindlimb representation area of the sensorimotor cortex.** (**A**, **B**) Schematic representation of somatosensory and motor cortex of the rat brain with expanded somatosensory and motor cortex [modified from (Tandon *et al.*, 2007)]. Red rectangle denotes the intended lesion area although the actual lesion area varied slightly among the rats. Vertical purple line indicates the bregma plane. Scales on the top and on the right side indicate the distance in mm rostrocaudally relative to the bregma and mediolaterally relative to the midline, respectively. (**C**) Macro anatomical image shows the lesion site in the right hemisphere. (**D**) Five consecutive Nissl-stained cortical sections with equal distance show the lesion site in two-dimension from the brain shown in **C**. Caudal is to the left and rostral is to the right for all the panels. Scale bar = 2 mm.

overnight post-fixation in the same fixative, the brain tissue was soaked in phosphate-buffered saline with 30% sucrose for 48 h, dissected into blocks which were then sliced into 50-µm sections with a freezing microtome. Every fourth Nissl-stained section across the lesion site was photographed and the rostrocaudal respective mediolateral extension as well as lesion volume were calculated.

## Analysis of HL-PA

The magnitude of postural asymmetry (MPA) and the side of the flexed limb were assessed as described previously (Bakalkin and Kobylyansky, 1989). Briefly, the measurements were performed under isoflurane anaesthesia, or in unanaesthetized decerebrate spinalized rats. The rat was placed in ventral decubitus (prone) position on a millimetre-grid paper sheet. To minimize effects of tactile stimulation during the analysis three threads were glued to the nails of the middle three toes of each limb. The fore or hindlimbs were gently pulled by the threads for 5–10 mm to reach the same level, then set free and the MPA was measured in millimetres as the length of the projection of the line connecting symmetric limb points (digits 2–4) on the longitudinal axis of the rat (Fig. 2A). The procedure was repeated six times in immediate succession, and the mean HL-PA value for a given rat was calculated and used in statistical analyses. For analysis in the supine position, the rat was placed in a V-shaped trough, a 90°—angled frame located on a levelled table surface with the 1-mm grid sheet; otherwise, the procedure was the same as for the prone position. The threshold of 2 mm that was the 94th MPA percentile in the sham rats was applied to define the asymmetric rats. A limb displaying shorter projection was regarded as flexed.

## Analysis of hindlimb resistance to stretch

Stretching force was analysed after spinal cord transection using the micromanipulator-controlled force meter device constructed in the laboratory. The resistance was measured as the amount of mechanical work $W_{Left}$ and $W_{Right}$ to stretch the left- and right hindlimbs, where W was stretching force integrated over stretching distance interval from 0 to 10 mm.

## EMG experiments

The EMG activity of the extensor digitorum longus (EDL), interrossei (Int) and peroneus longus (PL) muscles from both hindlimbs were recorded as described previously (Schouenborg *et al.*, 1992; Weng and Schouenborg, 1996).

## Analysis of gene expression

The rats were exposed to the left- or right-side UBI or the left- or right-side sham surgery (four groups; $n = 10$/

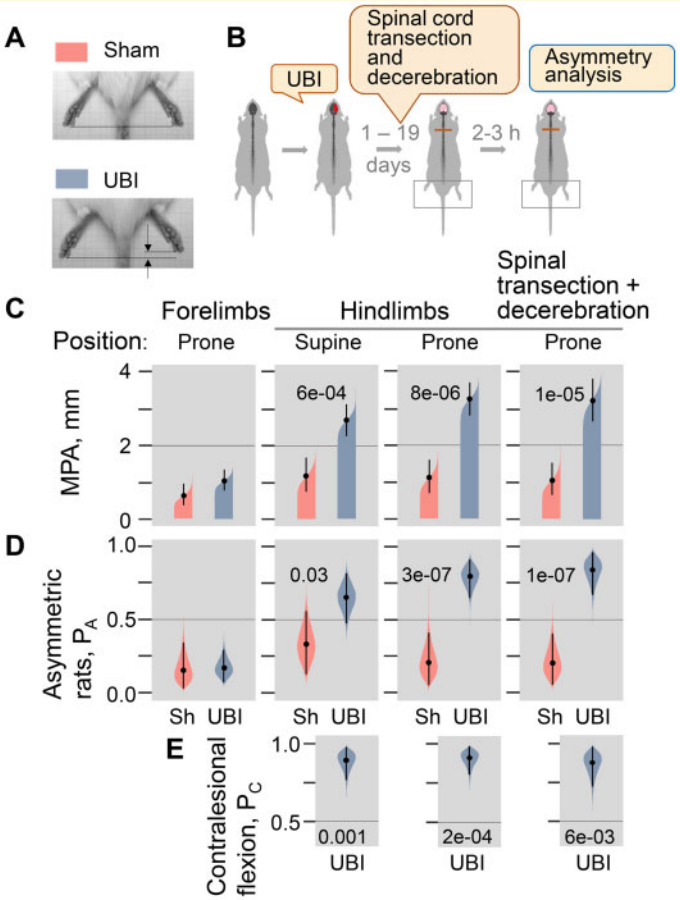


**Figure 2 The UBI-induced formation of HL-PA and its retention after complete spinal transection and decerebration.** (**A**) Analysis of HL-PA. The MPA was measured in millimetres as the length of the projection of the line connecting symmetric hindlimb distal points (digits 2–4) on the longitudinal axis of the rat. (**B**) Experimental design: postural asymmetry was analysed 2–3 h after spinalization in the rats exposed to the right-side UBI ($n = 27$ and 16 before and after transection and decerebration, respectively) or right-side sham surgery ($n = 11$) 1–14 days before the asymmetry analysis (for the number of rats at each experimental point, see also Supplementary Tables 1 and 3). A day of analysis within this observation period showed no time effects in statistical models. (**C**) The MPA after the UBI and sham surgery (Sh). Horizontal line denotes the 2 mm PA threshold that was 94th MPA percentile calculated for sham surgery group. (**D**) Probability of postural asymmetry ($P_A$; probability of a rat be asymmetric at MPA >2 mm) in the UBI group compared to the sham surgery group. (**E**) Probability of contralesional flexion ($P_C$) in asymmetric UBI animals. The MPA, $P_A$ and $P_C$ are plotted as median, 95% HPDCI, and posterior distribution from Bayesian regression. Adjusted *P*-values are shown if they are ≤0.05 for differences in MPA and $P_A$ between rat groups; and for difference in $P_C$ between the UBI group and the artificial 50% left/50% right flexion group of the same size. Differences were considered to be significant if 95% HPDCI did not include zero (see Supplementary Fig. 1), and adjusted *P*-values were ≤0.05.

group). The rats were sacrificed by decapitation on Day 3 after the injury, the lumbar spinal cords were dissected into the left and right halves. RNA purification, quality evaluation, cDNA synthesis and quantitative RT-PCR were described elsewhere (Kononenko *et al.*, 2018). mRNA levels of 13 neuroplastic genes (Supplementary Table 2) were normalized to geometric mean of expression levels of two control genes *Actb* and *Gapdh*.

## Statistical analysis

Postural asymmetry, stretching force and EMG data were analysed using Bayesian methods. Predictors and outcomes were centred and scaled before we fitted Bayesian regression models via full Bayesian framework by calling *Stan* 2.19.2 (Carpenter *et al.*, 2017) from *R* 3.6.1 R Core Team (2018) using the *brms* 2.10.0 (Burkner, 2017) interface. Models used Student's *t* response distribution with identity link function unless and had no intercepts with indexing approach to predictors (McElreath, 2020). Default priors were provided by the *brms* according to Stan recommendations (Gelman, 2019). Intercepts, residual SD and group-level SD were determined from the weakly informative prior student_t(3, 0, 10). *P*-values, adjusted using the multivariate *t* distribution with the same covariance structure as the estimates, were produced by frequentist summary in *emmeans* 1.4 (Searle *et al.*, 1980) together with the medians of the posterior

distribution and 95% highest posterior density continuous intervals (HPDCI). The asymmetry and contrast between groups were defined as significant if both 95% HPDCI did not include zero and adjusted *P*-value was $\leq 0.05$.

Differences in gene expression were assessed by two-way ANOVA (normally distributed data) or Kruskal–Wallis test of ranks (data with non-normal distribution). The Bonferroni procedure was used for multiple testing adjustments. *Post hoc* analysis was performed by Tukey's HSD test (normally distributed data).

For analysis of intra- and inter-regional gene co-expression patterns, Spearman's rank correlation coefficient was calculated for all gene pairs in each area ($N = 78$) and between the areas ($N = 169$). Sample size for each correlation coefficient was $n = 10$ animals. Statistical comparison of gene–gene coordination strength between the animal groups was performed using Wilcoxon signed-rank test to the set of absolute values of all correlation coefficients. Differences in the proportion of positive and negative correlations between animal groups were assessed using the Fisher's exact test with $2 \times 2$ contingency table.

Details are shown in Supplementary materials.

## Data availability

Data supporting the findings of this study are available within the article, its Supplementary material or upon request.

# Results

## Formation of postural asymmetry in UBI rats

In the first set of experiments, we examined whether the UBI induces formation of forelimb or HL-PA, whether the ipsi- or contralesional limb is flexed, and whether the asymmetry is retained after complete spinal cord transection and decerebration (Figs 1 and 2; Supplementary Fig. 1; Supplementary Tables 1, 3 and 4). The lesion produced by unilateral ablation by suction was confined to the hindlimb motor area (Fig. 1; Supplementary methods). The MPA, the probability to develop asymmetry ($P_A$), and the probability to flex the contralesional hindlimb ($P_C$) in the prone and supine positions were analysed 1–14 days after UBI or sham surgery. The UBI-induced asymmetry in hindlimb posture (HL-PA) was evident in anaesthetized animals before spinalization, and in unanaesthetized spinalized at high thoracic level and decerebrate rats (Fig. 2C). The hindlimb MPA was substantially (i.e. ~3-fold) higher in the UBI compared to sham-operated rats analysed before and after spinal cord transection and decerebration in the prone position; and before the transection and decerebration in the supine position. In the UBI group, correlations were significant between MPA analysed (i) before and after spinalization and decerebration in prone position; and (ii) in the prone and supine positions before these operations (Supplementary Table 4). The MPA in the UBI group was stable during the observation period from the 1st to 19th day after the injury; a day of measurement included as confounder in statistical models showed no time effects. No apparent forelimb asymmetry was developed.

The rats showing a MPA >2 mm were regarded as asymmetric; the 2 mm threshold corresponded to the 94th percentile of hindlimb MPA in the sham surgery group (Fig. 2; Supplementary Fig. 1). The $P_A$ was significantly higher in the UBI rats compared to the sham-operated animals when they were analysed before and after spinal cord transection and decerebration in the prone position; and before these operations in the supine position (Fig. 2D). The $P_C$ for asymmetric UBI rats was significantly greater than 50% contra-/50% ipsilesional flexion ratio for the prone position before and after transection and decerebration; and for the supine position before these operations (Fig. 2E). Figure 2 shows data for the right-side UBI; the left-side UBI similarly produced HL-PA with contralesional hindlimb flexion (MPA, $P_A$ and $P_C$ did not differ between the left- and right-side UBI groups: $n = 10$ and 16, respectively; $P > 0.4$ for rat groups analysed either in the prone or supine positions, and either before or after spinalization). Thus the unilateral focal injury to the hindlimb representation area of the sensorimotor cortex resulted in formation of the HL-PA with contralesional flexion whereas forelimbs were not apparently affected. The asymmetry persisted after spinalization and decerebration suggesting that the UBI-induced spinal neuroplastic response underlies HL-PA maintenance.

## Effects of deafferentation and neuromuscular signalling blockade on HL-PA

We next sought to determine whether afferent somatosensory input is required for the HL-PA formation in the UBI rats. The HL-PA was analysed before and after bilateral rhizotomy from the L1 to S2 spinal levels in the spinalized rats received earlier either the left- or right-side UBI. After the left-side UBI, the MPA and $P_A$ were strongly, 9.0- and 3.6-fold, respectively, reduced after rhizotomy (Fig. 3A–C; Supplementary Figs 2 and 3). In contrast, in the right-side UBI rats the MPA and $P_A$ remained stable after rhizotomy and were substantially, 8.0- and 2.6-fold, respectively, higher than those in the left-side UBI group. These data suggest that the HL-PA maintenance in spinalized rats may depend on (i) afferent somatosensory input after the left-side UBI, and on (ii) activity of motoneurons signalling to hindlimb muscles or changes in neuromuscular system after the right-side injury.

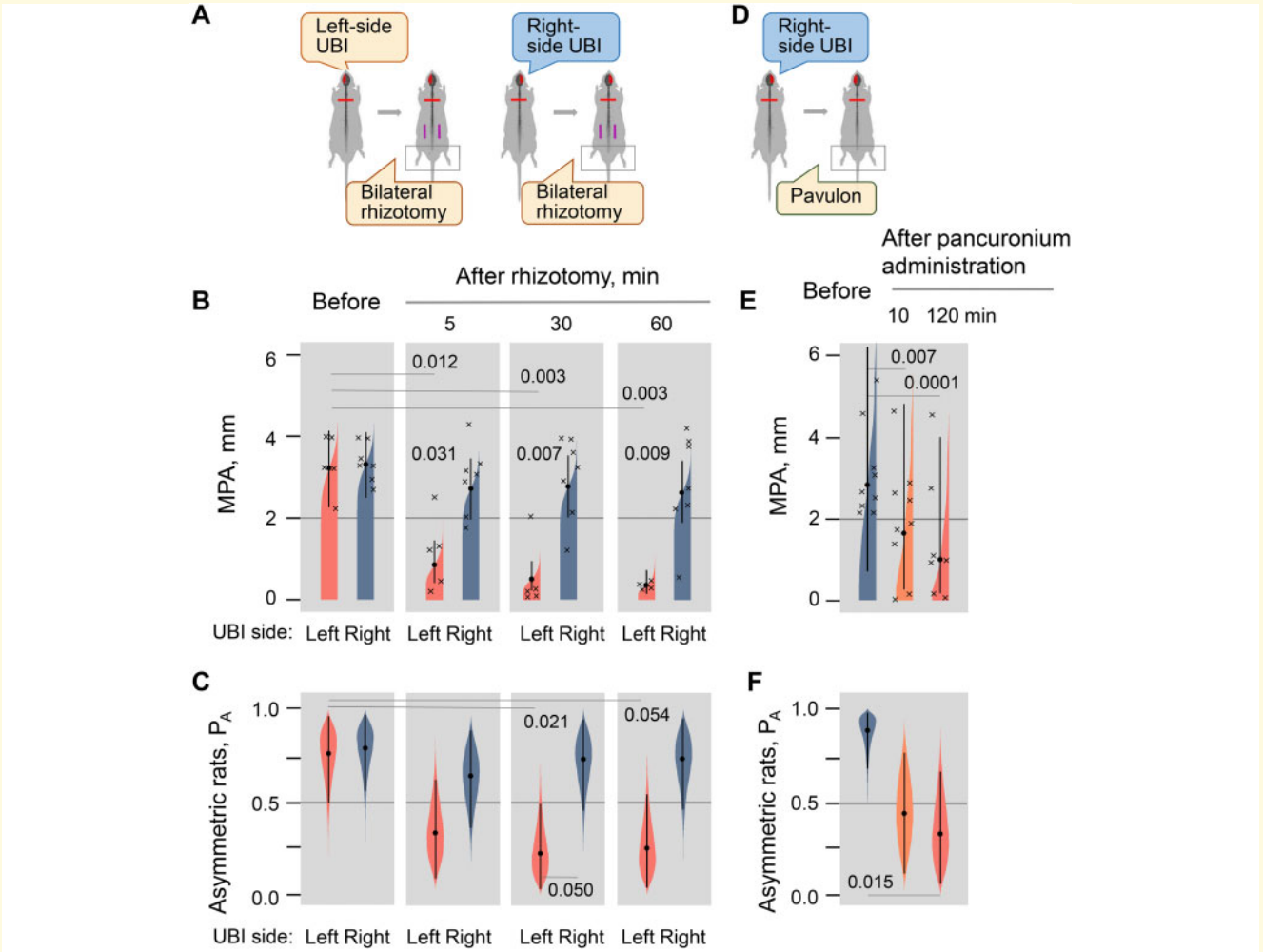


**Figure 3 Effects of deafferentation and pancuronium, a curare-mimetic muscle relaxant on the HL-PA.** (**A–C**) Effects of bilateral rhizotomy from the L1 to S2 spinal levels on MPA and $P_A$ in spinal UBI rats. Animals were exposed to the left-side ($n = 5$) or right-side ($n = 7$) UBI, and after 3–19 days later they were spinalized and then after 1 h subjected to bilateral rhizotomy. HL-PA was analysed before and 5, 30 and 60 min after the rhizotomy. (**D–F**) Analysis of HL-PA before ($n = 9$) and 10 ($n = 9$) and 120 ($n = 7$) min after pancuronium infusion. HL-PA was analysed 3–12 days after the right-side UBI in prone position. Differences were considered to be significant if 95% HPDCI did not include zero (see Supplementary Figs 2–4), and adjusted *P*-values were $\leq 0.05$. For details, see legend to Fig. 2.

To examine whether the HL-PA induced by the right-side UBI is maintained by central or peripheral (neuromuscular) mechanism, pancuronium (pavulon), a curare-mimetic muscle relaxant was administered in rats displaying HL-PA to block the neuromuscular junction (Fig. 3D–F; Supplementary Fig. 4). Pancuronium infusion in the anaesthetized rats that received the right-side UBI 3 days before the experiment, resulted in rapid decrease of the MPA and then completely abolished HL-PA. The MPA was stable in UBI rats given saline for at least 120 min ($n = 9$).

## Stretching resistance analysis

We next studied whether the UBI may differently affect biomechanical properties of the contra- and ipsilesional hindlimbs by analysing the passive hindlimb musculo-articular resistance to stretching in the anaesthetized spinalized rats using the micromanipulator-controlled force meter device (Fig. 4). The asymmetry in the resistance was assessed using (i) the left/right asymmetry index for the work (W), $AI_W = \log_2 (W_{Left}/W_{Right})$, where $W_{Left}$ and $W_{Right}$ were the W applied to stretch the left- and right hindlimbs (Fig. 4D and E); and (ii) the index for difference in the work between the left- and right hindlimbs $\Delta W = (W_{Left} - W_{Right})$ (Fig. 4F and G). The indexes were integrated for a 10-mm stretching distance. Both the $AI_W$ and $\Delta W$ were statistically analysed because they may depend differently on the resistance force and the distance over which they are stretched.

The right (contralesional) versus left (ipsilesional) hindlimb demonstrated greater resistance after the left-side

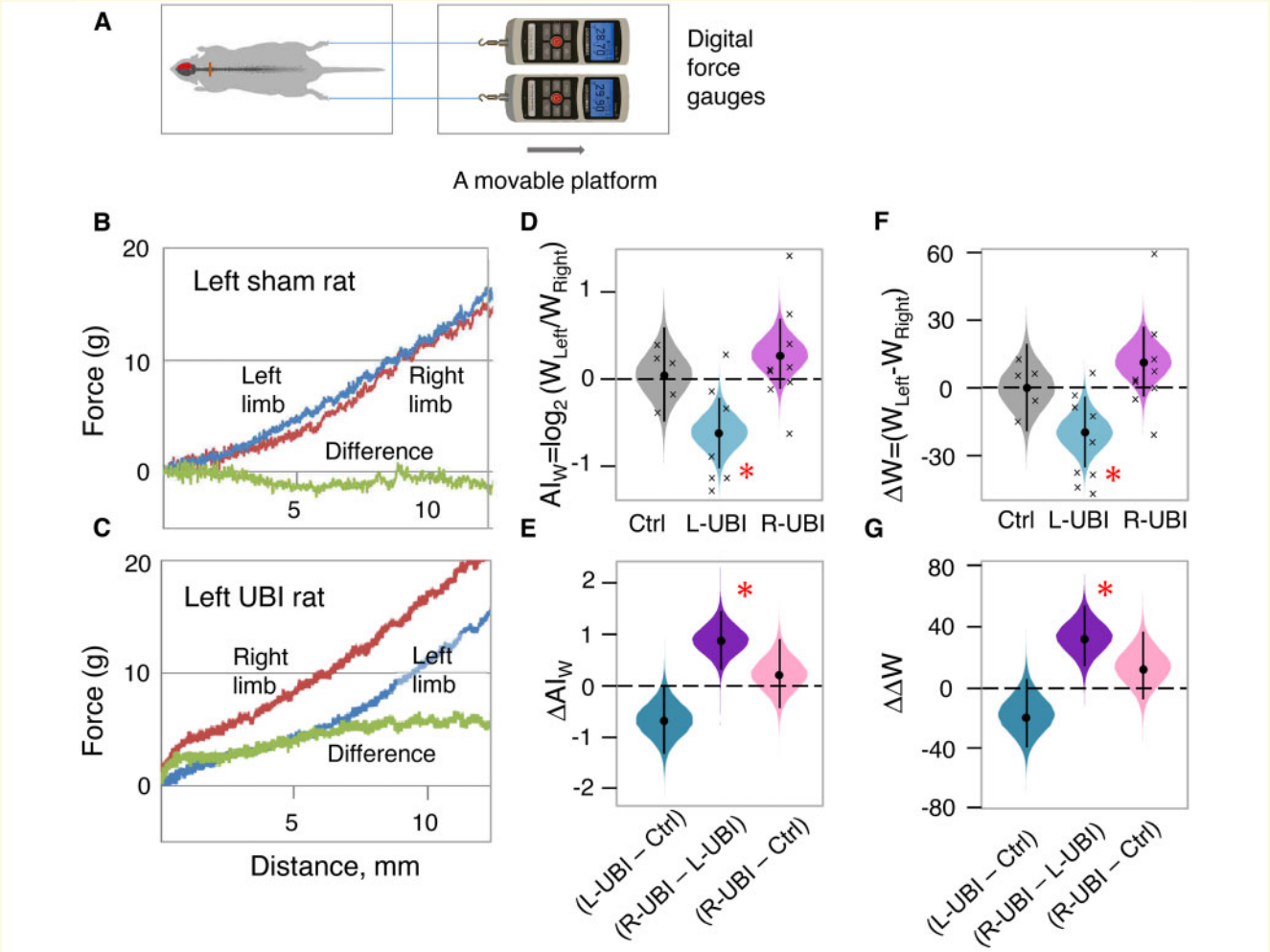


**Figure 4 Effects of the UBI on stretching resistance of the contra- and ipsilesional hindlimbs.** (**A**) Experimental setup. The micromanipulator-controlled force meter device constructed in the laboratory consisted of two digital force gauges fixed on a movable platform operated by a micromanipulator. The rat was placed in prone position on a thermostatically controlled heating pad. Two silk threads were hooked to the force gauges and their other ends were glued to the nails of the middle three toes of both hindlimbs. The legs were placed in symmetric position and stretched for the 10 mm distance at 1 mm/s speed. Resistance was analysed as the amount of mechanical work W to stretch a hindlimb, calculated as integral of stretching force over 0–10 mm distance. (**B**, **C**) Raw representative data show traces of the stretching force recorded from the left and right hindlimbs of the left sham and left UBI rats. Stretching force was analysed in the spinal rats that received left-side ($n = 9$) or right-side ($n = 9$) UBI, and spinal control rats ($n = 5$) in 6–10 days after brain injury or sham surgery. (**D, E**) The UBI effects were analysed as changes in asymmetry index $AI_W = \log_2 (W_{Left}/W_{Right})$ and (**F, G**) difference in stretching force between the left and right hindlimbs $\Delta W = (W_{Left}—W_{Right})$ in gm × mm. Medians, 95% HPDCI and densities are shown. Differences of the $AI_W$ (**D**) and ΔW (**F**) from zero, and differences between UBI and control (Ctrl) groups in the $AI_W$ ($\Delta AI_W$) (**E**) and ΔW (ΔΔW) (**G**) were assessed in Bayesian framework and are reported as significant if their 95% HPDCI did not include zero and adjusted *P*-values were ≤0.05 (shown by *).

UBI (Fig. 4D and F). The produced changes were significant in both the $AI_W$ [median of the posterior distribution as estimate (median) = −0.611, 95% HPDCI = (−1.023, −0.216), adjusted *P*-value (*P*) = 0.008, the Left to Right ratio in resistance or L/R ratio = 0.65] and ΔW [median = −19.684, 95% HPDCI = (−35.230, −3.840), $P = 0.040$]. No statistically significant asymmetry was evident in the right-side UBI and control groups, albeit the median levels of both the $AI_W$ and ΔW in the right-side UBI rats exceeded those in the control group. Resistance was significantly different between the left- and right-side UBI groups in both the $AI_W$ [median = 0.889, 95% HPDCI = (0.313, 1.454), $P = 0.006$, L/R ratio was 1.85-fold larger for right-side UBI] (Fig. 4E) and the ΔW [median = 31.307, 95% HPDCI = (9.070, 53.384), $P = 0.015$] (Fig. 4G).

## UBI effects on hindlimb NWRs

Along with changes in posture, the UBI may differentially affect the NWRs of the contra- and ipsilesional hindlimbs producing an asymmetric pattern. We addressed this

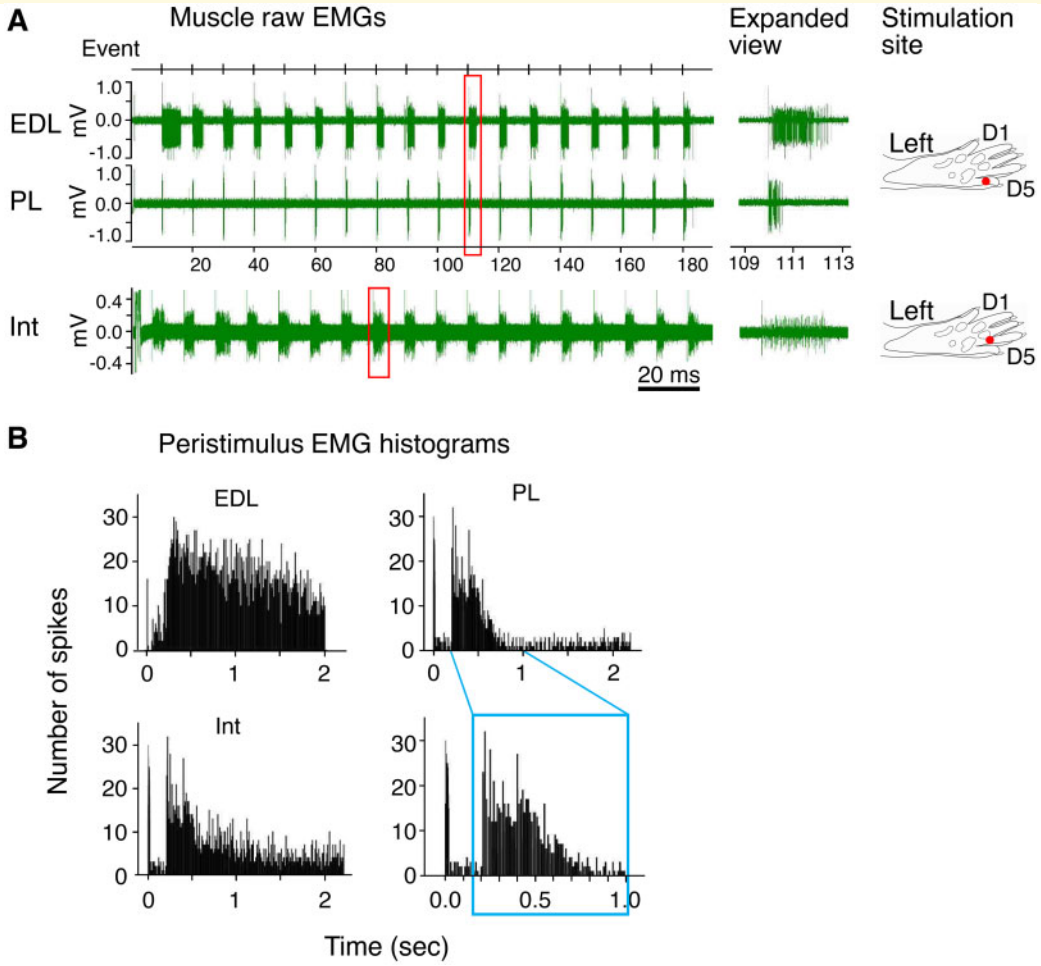


**Figure 5 EMG examples and respective stimulation sites of three muscles of the UBI rats.** (**A**) Left: EMG responses of the the extensor digitorum longus EDL, peroneus longus (PL) and interossei (Int) muscles to 18 electrical stimulations. Middle: Expanded view of the EMG spikes from the regions delimited by the rectangles. Right: Stimulation sites. (**B**) Peristimulus histogram of these muscles from 16 stimulations (2–17). Blue rectangle shows the time window (0.2–1.0 s) for the area analysed statistically.

question by analysis of the hindlimb NWRs evoked by electrical stimulation of symmetric digit spots on left and right hind paws, and recorded using EMG techniques in unanaesthetized UBI rats after their decerebration and complete spinal cord transection (Figs 5 and 6; Supplementary Tables 1 and 5). EMG responses were recorded from the EDL, Int and PL muscles of the contra- and ipsilesional hindlimbs in the rats exposed to the left- or right-side UBI, and the left- or right-side sham surgery (Figs 5 and 6). EMG activity was recorded in response to 18 stimulations (Fig. 5A); most responses were stable across the stimulation train, however, wind-up was sporadically observed. Peristimulus histograms denote that a main fraction of the responses was recorded in the 0.2–1.0 s interval. This fraction was included in statistical analysis (Fig. 5B) and was likely elicited through activation of the C-fibres.

Stimulation thresholds (Thr) and the number of spikes (SN) of EMG responses to current stimulation were compared between the left and right limbs using the Left/Right asymmetry index [AI = $\log_2$(L/R), were L and R were values for the left- and right-side muscles] for the threshold ($AI_{Thr}$) or the spike number ($AI_{SN}$) (Fig. 6D–G; the number of analysed animals is shown in Supplementary Table 5). No asymmetry in the sham surgery and UBI groups, and no significant differences between the groups were revealed for the threshold values (Fig. 6D and F). Analysis of the sham surgery groups revealed significant asymmetries of EMG responses in the number of spikes for the EDL in the right-side sham surgery group [median = −1.088, 95% HPDCI = (−1.898, −0.265), $P = 0.034$, L/R ratio = 0.47] and for the Int in the left-side sham group [median = −1.914, HPDCI = (−3.070, −0.725), $P = 0.005$, L/R ratio = 0.27] (Fig. 6E). The median $AI_{SN}$ of each of these muscles in each the left and right sham group was less than zero. Analysis of the combined sham surgery group demonstrated that the number of spikes was higher on

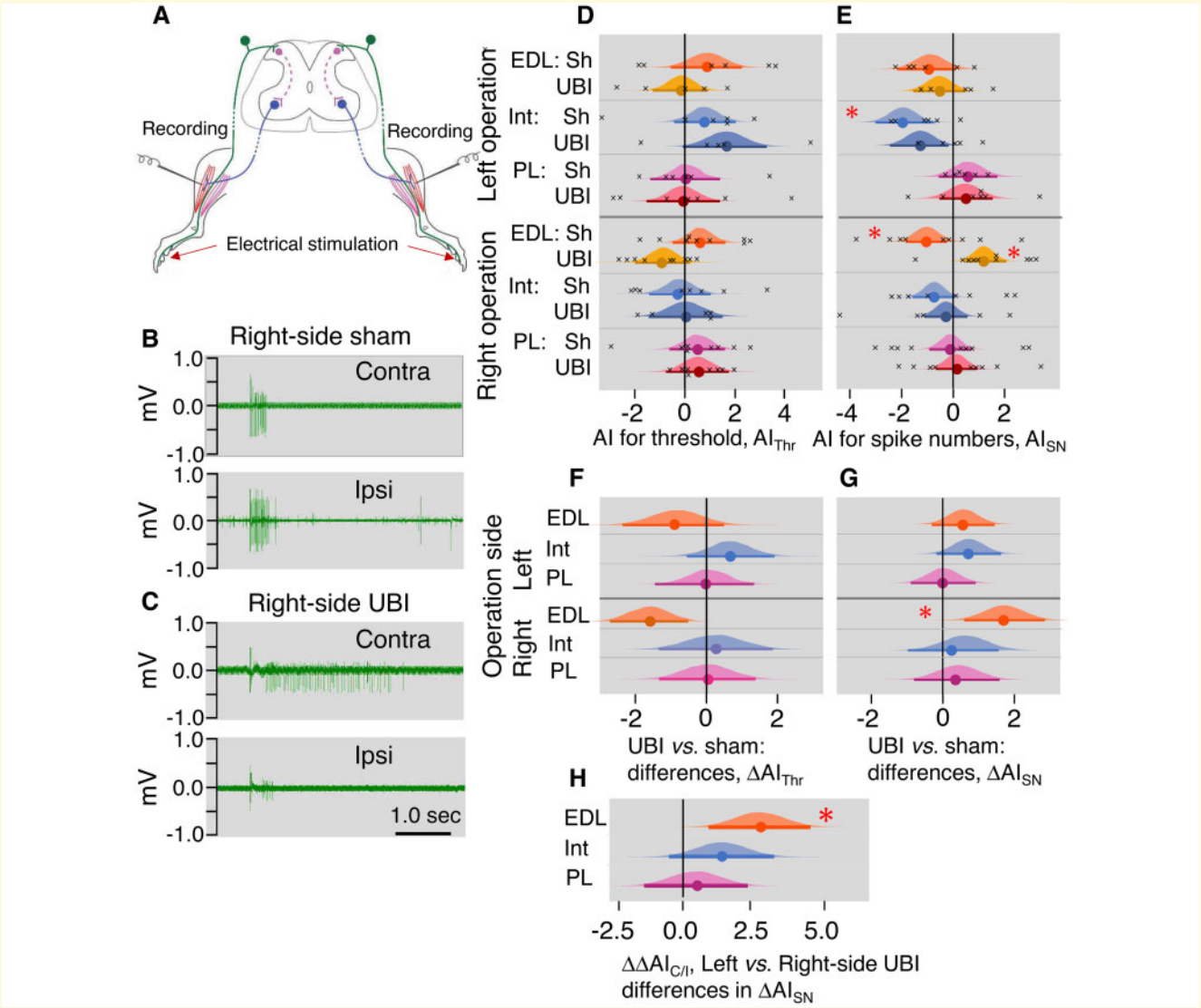


**Figure 6 Effects of the left- and right-side UBI on the left/right asymmetry index for the stimulation threshold ($AI_{Thr}$) and the spike number ($AI_{SN}$) of the EDL, Int and PL muscles.** (**A**) Experimental design. The rats with UBI or sham surgery were spinalized and decerebrate. Analysis of EMG activity of left and right hindlimb muscles evoked by electrical stimulation of symmetric digit spots on left and right hind paws was initiated ~3 h after spinalization and decerebration. For the number of rats see Supplementary Tables 1 and 5. Altogether 38 rats including 6 left-side sham, 11 right-side sham, 7 left-side UBI and 14 right-side UBI rats were analysed between 3rd and 14th day after UBI or sham surgery. All 11 right-side sham-operated rats, and 14 right-side UBI rats constituted the rat groups in the EMG experiment were analysed for development of HL-PA (shown in Fig. 2) before the EMG experiment. The NWRs of the left and right limbs were stimulated and recorded ipsilaterally. (**B, C**) Representative examples of EMG responses of the EDL muscle to electrical stimulation of digit 4 of the right-side sham and right-side UBI rats. (**D, E**) The Left/Right asymmetry index for threshold ($AI_{Thr} = \log_2[Thr_{Left}/Thr_{Right}]$, where Left and Right were values for the left and right side) and the spike number ($AI_{SN} = \log_2[(1+SN_{Left})/(1+SN_{Right})]$). (**F, G**) Difference between the UBI and sham groups ($\Delta AI = (AI_{UBI} - AI_{sham})$) in $AI_{Thr}$ and $AI_{SN}$. (**H**) Difference in the $AI_{SN}$ magnitude between effects of the left-side and right-side UBI. The difference was assessed using the contra/ipsi AI [$AI_{C/I} = \log_2(C/I)$, where C and I are the number of spikes of the contra and ipsilesional muscles]. Data are shown as $\Delta\Delta AI_{C/I} = [(AI_{C/I,\ R\text{-}UBI} - AI_{C/I,\ R\text{-}sham}) - (AI_{C/I,\ L\text{-}UBI} - AI_{C/I,\ L\text{-}sham})]$. Medians, 95% HPDC intervals and densities of posterior estimates from Bayesian sampler are plotted. Asymmetry and contrast between the UBI and sham groups were defined as significant (shown by *) if 95% HPDC intervals for $AI_{Thr}$ or $AI_{SN}$ did not include zero, and adjusted *P*-values were $\leq 0.05$.

the right compared to the left side [EDL: median = −1.049, 95% HPDCI = (−1.693, −0. 418), $P = 0.007$; Int: median = −0.923, 95% HPDCI = (−1.581, −0.236), $P = 0.040$)].

After the brain injury, significant asymmetry in the number of evoked spikes was identified for the EDL muscle in the right-side UBI rats [median = 1.147, HPDCI = (0.356, 1.910), $P = 0.015$, L/R ratio = 2.2]

(Fig. 6E). Representative examples of the UBI-induced asymmetry for the EDL muscle is shown on Fig. 6B and C. The UBI and sham surgery groups were significantly different in the $AI_{SN}$ the EDL after the right-side injury [median = 2.238, HPDCI = (1.111, 3.354), $P = 0.001$, 4.7-fold difference in the L/R ratio] (Fig. 6G). No significant differences were revealed after the left-side UBI.

We next assessed whether the magnitude of the injury-induced changes in the spike number asymmetry significantly differs between the left- and right-side UBI using the contra/ipsilesional asymmetry index $AI_{C/I}$ = [$AI_{C/I}$ = $\log_2(C/I)$], where C and I were the number of spikes of the contra and ipsilesional muscles. Differences between effects of the right-side UBI [$\Delta AI_{C/I,R}$ = ($AI_{C/I,R\text{-}UBI}$—$AI_{C/I,R\text{-}sham}$)] and left-side UBI [$\Delta AI_{C/I,\ L}$ = ($AI_{C/I,L\text{-}UBI}$—$AI_{C/I,L\text{-}sham}$)] were computed as $\Delta\Delta AI_{C/I}$ = ($\Delta AI_{C/I,R}$—$\Delta AI_{C/I,L}$) (Fig. 6H). The Bayesian analysis demonstrated that the ratio of the $AI_{C/I}$ for the right-side UBI to the $AI_{C/I}$ for the left-side UBI is significantly greater compared to the ratio of the $AI_{C/I}$ for the right-side sham surgery to the $AI_{C/I}$ for left-side sham surgery for the EDL muscle [median = 2.793, HPDCI = (0.890, 4.624), $P = 0.003$, 6.9-fold difference].

In summary, the EDL and Int NWRs were found to be lateralized with higher responses of the right versus left hindlimb muscles in sham rats. On this asymmetric background, the right-side UBI-induced asymmetric changes in the EDL due to its preferential activation on the contralesional versus ipsilesional side. No significant asymmetric responses were revealed after the left-side UBI. Effects of the left-side and right-side UBI on the EDL muscle were significantly different in the $AI_{C/I}$ magnitude.

## UBI effects on expression of neuroplasticity genes, and their intra- and inter-regional co-expression patterns in lumbar spinal cord

The HL-PA and asymmetry in the NWRs may persist after spinalization and decerebration due to the UBI-induced neuroplastic response in the lumbar spinal domains underlined by changes in gene expression. We assessed whether the left- and right-side UBI affects expression of 13 neuroplasticity genes that were *Arc*, *Bdnf*, *cFos*, *Dlg4*, *Egr1*, *Homer-1*, *Gap43*, *GluR1*, *Grin2a*, *Grin2b*, *Nfkbia*, *Syt4* and *Tgfb1* in the left and right halves of the lumbar spinal cord analysed as a readout of neuroplastic response. Four groups including the left- and right-side UBI, and the left- and right-side sham surgery groups were analysed. Two-way ANOVA with operation type (UBI versus sham) and measurement side (left versus right) as factors revealed significant differences between UBI and sham surgery groups for *Grin2a* (*P* adjusted by Bonferroni correction, adj. $P = 0.0004$), *Tgfb1* (adj. $P = 0.0023$) and *Dlg4* (adj. $P = 0.019$), and between measurement sides for *Grin2b* (adj. $P = 0.037$). The left- and/or right-side UBI resulted in a downregulation of *Grin2a* (*post hoc* test: left-side UBI, $P = 0.0007$; right-side UBI, $P = 0.028$) and *Dlg4* (left-side UBI, $P = 0.0007$), and upregulation of *Tgfb1* (left-side UBI, $P = 0.002$; right-side UBI, $P = 0.025$) (Fig. 7A–C). *Grin2b* demonstrated higher expression in the left half compared to the right half of the spinal cord (*post hoc* test: $P = 0.0029$) (Fig. 7D) that was replicated by analysis of intact animals ($n = 10$; paired *t*-test: $P = 0.0001$) (Fig. 7E).

Gene co-expression patterns characterize regulatory interactions within and across tissues (or CNS areas) (Dobrin *et al.*, 2009; Long *et al.*, 2016). We examined whether UBI affects gene–gene (i) inter-area correlations between the left and right halves of the lumbar spinal cord, and (ii) intra-area correlations in these halves. The inter-area positive correlations dominated in both the left and right sham surgery groups, while their proportion was reduced after the UBI; the effect was statistically significant after the left ($P = 5.8 \times 10^{-7}$) (Fig. 7F and H), but not right-side brain injury ($P = 0.081$) (Fig. 7G and I). Proportion of the intra-area positive correlations was decreased after the UBI in the left (left-side injury: $P = 7.7 \times 10^{-4}$; right-side injury: $2.0 \times 10^{-3}$) and right (left-side injury: $P = 1.4 \times 10^{-4}$; right-side injury: $4.1 \times 10^{-4}$) halves of lumbar spinal cord (Supplementary Fig. 5). Furthermore, the coordination strength of gene co-expression patterns was significantly decreased after the left UBI in the contralesional (right side) lumbar domain ($P = 1.8 \times 10^{-11}$) but not in the ipsilesional (left side) domain (Supplementary Fig. 5); effects of the right-side UBI were not significant.

Thus the UBI induced changes in expression of neuroplasticity genes and impaired coordination of their expression between and within the ipsi- and contralesional halves of lumbar spinal segments; the effects were more pronounced after the left-side compared to the right-side brain injury.

# Discussion

The principal findings of this study are the formation of the HL-PA with flexion on the contralesional side, and the asymmetric changes in hindlimb NWRs and in resistance to stretching, all induced by the unilateral focal injury to the hindlimb representation area of sensorimotor cortex. These effects were evident in the rats spinalized at the high thoracic level suggesting the brain injury-induced rearrangement of lumbar spinal circuits prior to the transection. This notion is supported by the UBI-induced changes in expression and co-expression patterns of neuroplasticity genes in the lumbar spinal cord. Peripheral biomechanical mechanisms may likely be excluded because HL-PA was blocked by pancuronium. Formation of the contralesional flexion along with higher resistance to stretching and activation of NWRs on the contralesional

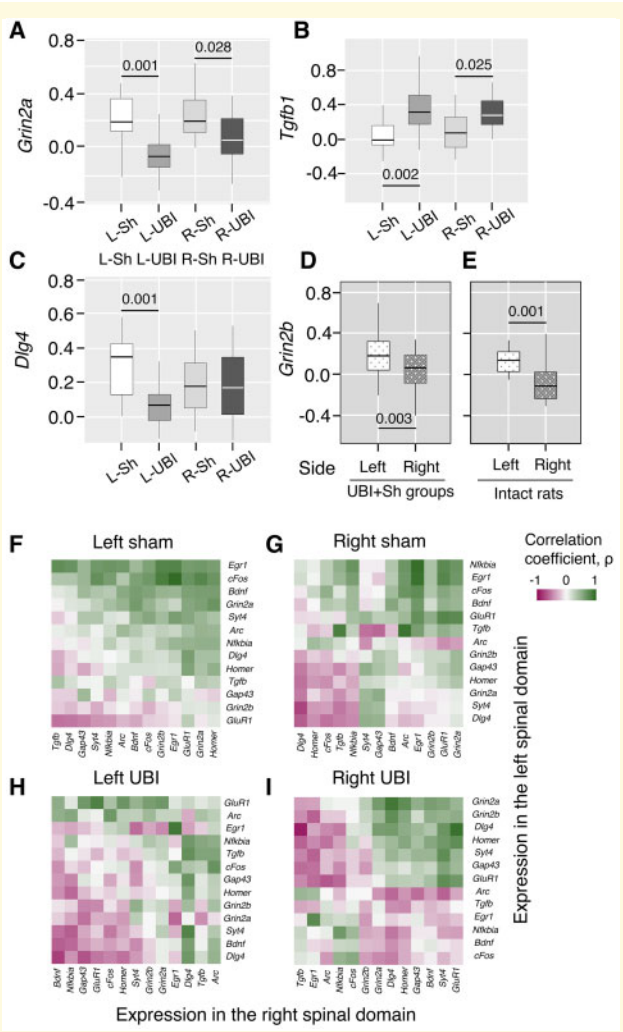


**Figure 7 Expression of neuroplasticity genes (A–C), lateralized expression (D, E), and inter-area co-expression patterns (F–I) in the lumbar spinal cord of the rats exposed to the left- and right-side UBI or sham surgery.** Four groups of rats ($n = 10$/group) were sacrificed on Day 3 after the injury for tissue dissection. Shown are $\log_2$-transformed levels of *Grin2a* (**A**), *Tgfb1* (**B**), *Dlg4* (**C**) and *Grin2b* (**D**, **E**) mRNAs in the lumbar spinal cord. In (**A**–**C**), L- and R- stand for the left- and right-side UBI or sham surgery. In (**D** and **E**), Left and Right denote the left and right spinal half. In (**D**), the data combined for two UBI and two sham surgery groups ($n = 40$) and *post hoc P* are shown; these four groups did not differ between each other in the *Grin2b* expression in either the left or right domain; therefore, the data were pooled for statistical analysis. (**E**) Data for intact rats ($n = 10$) and *P*-value for left–right difference (paired *t*-test). The horizontal line in the box represents the median; the box hinges represent the first (Q1) and third quartiles (Q3). Upper and lower whiskers extend from the hinge to the highest/lowest value that lies within the 1.53 interquartile range (IQR) of the hinge. Adjusted *P*-values are shown. (**F–I**) Heatmaps with Spearman coefficients for correlations in expression levels between the left and right lumbar domains for all gene pairs in the left- (**F**) and right- (**G**) side sham operation, and the left- (**H**) and right- (**I**) side UBI groups.

side suggest that neuroplastic changes in the spinal cord are caused by asymmetric activity of pathways that decussate the midline.

The ipsilateral hindlimb flexion was induced by hemicerebellar lesion (DiGiorgio, 1929, 1942; Alella, 1948; Chamberlain *et al.*, 1963; Patterson, 2001), or hemilabyrinthectomy (Straka and Dieringer, 1995). In contrast, contralesional hindlimb flexion was developed after a focal injury of the hindlimb representation area of the sensorimotor cortex (although a small part of the hindlimb somatosensory cortex might have been aspirated in some rats as also was described elsewhere (Tandon *et al.*, 2007)) or large injury of one hemisphere ((Varlinskaia *et al.*, 1984; Vartanyan and Klementiev, 1991) and the present work). Search for neurotransmitter system involved in HL-PA formation demonstrated that opioid peptides and synthetic opioids (Bakalkin *et al.*, 1980; Chazov *et al.*, 1981; Bakalkin *et al.*, 1986; Bakalkin and Kobylyansky, 1989) along with Arg-vasopressin (Klement'ev *et al.*, 1986; Lukoyanov *et al.*, 2018) may induce HL-PA in spinalized animals. The striking finding was that the response to administration of these substances was developed either on the left or right side of the body. The $\kappa$-opioid agonists dynorphin and bremazocine induced flexion of the left hindlimb, while $\delta$-agonist Leu-enkephalin and Arg-vasopressin caused the right hindlimb to flex. Release of the endogenous opioid peptides in rats exposed to stress or pain stimuli also produced HL-PA, which was blocked by administration of the opioid antagonist naloxone (Bakalkin *et al.*, 1982). These side-specific neurohormonal mechanisms may potentially mediate formation of the left or right hindlimb flexion after UBI.

The right-side UBI-induced HL-PA was resistant to bilateral deafferentation suggesting that spinal reflexes do not contribute to asymmetry formation. In contrast, bilateral lumbar rhizotomy after the left-side UBI abolished HL-PA that thereby may be developed due to differences between reflexes on the contra- and ipsilesional sides. In the course of the asymmetry analysis, no nociceptive stimulation was applied and tactile stimulation was negligible; the legs were stretched by pulling the threads glued to nails of the toes. The HL-PA magnitude was the same and correlated between the supine and prone positions for which effects of tactile stimulation, if any, should be different. Application of lidocaine on the toes, which were pulled at the stretching, did not affect the asymmetry formation (unpublished data). It was firmly established that the stretch and postural limb reflexes are abolished immediately and for days after complete spinal cord transection (Miller *et al.*, 1996; Musienko *et al.*, 2010; Frigon *et al.*, 2011) and substantially decreased under anaesthesia (Zhou *et al.*, 1998; Fuchigami *et al.*, 2011). Therefore, the NWRs and stretch reflex likely do not contribute to HL-PA formation and/or its

maintenance in the preparations of the unanaesthetized decerebrate spinalized UBI rats, and spinalized UBI rats under anaesthesia analysed in the present study. On the other hand, responses mediated by the Group II muscle afferents may remain active after spinalization in acute experiments (Jankowska, 1992; Valero-Cabre *et al.*, 2004; Lavrov *et al.*, 2015). Together with these observations, our findings suggest that the HL-PA is a complex phenomenon that is developed either due to (i) a persistent asymmetric activity of lumbar motoneurons not stimulated by afferent input; or due to (ii) discharge of proprioceptive neurons activated perhaps by Group II muscle afferents, which are tonically active and maintain muscle tone. These two mechanisms may differentially contribute to formation of the left and right hindlimb flexion. The second mechanism is supported by human studies demonstrated that the Group II muscle afferents are involved in the exaggerated reflexes in spastic hemiplegic and paraplegic patients (Eriksson *et al.*, 1996; Marque *et al.*, 2001).

Our data indicate that NWRs of EDL and Int muscles are lateralized in control animals. On this left-right asymmetric background, the left- and right-side brain lesions were not mirror symmetric in their effects on the hindlimb NWRs. After the right-side UBI, sign of the $AI_{SN}$ for the EDL was changed from minus to plus, but the NWR was still significantly asymmetric—different from zero. Thus, the right-side UBI resulted in greater activation of withdrawal EDL responses on the left (contralesional) side compared to the right (ipsilesional) side. The left-side UBI did not produce significant changes in the EDL, Int and PL NWRs. Muscles which may be affected by the left-side injury remain to be identified. The NWRs have a modular organization in which each module controls a single or a few synergistic muscles and each module performs a comprehensive and functionally adapted sensorimotor transformation resulting in appropriate activation of the target muscle(s) (Schouenborg, 2002). Effects of the left- and right-side UBI may be interpreted in the context of this mechanism; different sets of NWR modules may be targeted by the left- and right-side brain injury.

Dependence of the right hindlimb flexion formation on afferent stimulation corroborates asymmetry of mono- and polysynaptic segmental reflexes in intact rats and cats (Hultborn and Malmsten, 1983*a*, *b*; Malmsten, 1983) and asymmetry of NWRs in control rats, which all display greater activity on the right body side. The uncovered lateralization in the spinal cord may be relevant as the physiological basis for several neurological phenomena differently developed after injury to the left and right hemisphere (see Introduction section; Spinazzola *et al.*, 2003; Fernandes *et al.*, 2018). The hemisphere specific motor effects laid the basis for the general concept of motor lateralization in which the left hemisphere assures mechanical efficiency under predictable conditions, while the right hemisphere imparts robustness under unpredictable situations (Sainburg, 2014). Our results are in line with the motor lateralization concept. They suggest that the left hindlimb motor cortex might enable tonic, afferent stimulation independent control of the right hindlimb postural responses while its lesion eliminates this function. Complementarily, the right cortex might control the afferent-dependent postural reactions of the left hindlimb, and its injury could diminish segmental reflex-mediated motor responses.

Besides left–right differences in segmental reflexes (Hultborn and Malmsten, 1983*a*, *b*; Malmsten, 1983; and this study), physiological, anatomical and molecular asymmetries in the spinal cord (Bakalkin *et al.*, 1980; Chazov *et al.*, 1981; Bakalkin *et al.*, 1986; Bakalkin and Kobylyansky, 1989; Nathan *et al.*, 1990; de Kovel *et al.*, 2017; Kononenko *et al.*, 2017; Ocklenburg *et al.*, 2017; Kononenko *et al.*, 2018; Woytowicz *et al.*, 2018) along with general lateralization of motor functions (Sainburg, 2014; Sainburg *et al.*, 2016; Knebel *et al.*, 2018; Stancher *et al.*, 2018) have been reported. Three-quarters of cervical spinal cords are asymmetric with larger right side (Nathan *et al.*, 1990). Spinal neural circuits controlling activity of the left and right hindlimb muscles may be differentially affected by opioid agonists (Bakalkin *et al.*, 1980; Chazov *et al.*, 1981; Bakalkin *et al.*, 1986; Bakalkin and Kobylyansky, 1989). Expression of opioid receptors is lateralized in the spinal cord, while their inter-regional co-expression patterns are side-specific and intra-regional (between the dorsal and ventral domains) co-expression profiles are differently affected by the left- and right-side body injury (Kononenko *et al.*, 2017). In human embryos transcriptional maturation rates are different between left and right spinal cord suggesting that spinal cord lateralization is not directed from the forebrain (de Kovel *et al.*, 2017). The present study demonstrates that the *Grin2b* gene coding for the NMDA receptor subunit, which is involved in circuit formation and synaptic plasticity, is expressed at higher levels in the left compared to the right lumbar spinal cord. Interestingly, the lateralized expression of this gene underlies structural and functional left–right asymmetries in the hippocampus (Kawakami *et al.*, 2003; Wu *et al.*, 2005; Kohl *et al.*, 2011).

Expression of the *Grin2a*, *Dlg4* and *Tgfb1* neuroplasticity genes in the lumbar spinal segments was altered after the unilateral brain lesion. The *Grin2a* subunit of the glutamate receptors regulates formation of neural circuits and their plasticity. The *Dlg4* gene codes for PSD95 involved in AMPA receptor-mediated synaptic plasticity and post-NMDA receptor activation events (Won *et al.*, 2016). *Tgfb1* gives rise to transforming growth factor $\beta 1$ regulating inflammation, expression of neuropeptides and glutamate neurotoxicity (Buisson *et al.*, 2003; Santibanez *et al.*, 2011). The glutamate receptors may modulate spinal NWRs (You *et al.*, 2004) and flexion response in a model of spinal learning (Joynes *et al.*, 2004), and mediate HL-PA formation induced by electrical limb

stimulation (Anderson and Winterson, 1995). These findings suggest that glutamate receptors may have a role in the UBI-induced formation HL-PA and modifications of hindlimb NWRs.

Remarkably the co-expression patterns of neuroplasticity genes were strongly dysregulated after the UBI as follows from the decline in the coordination strength and decrease in the proportion of positive inter- and intra-area correlations. Robust changes in the inter- and intra-regional gene co-expression patterns is a novel phenomenon suggesting that the UBI abolishes coordination of gene expression between the left and right halves of anatomically symmetric spinal cord, and within each of these halves.

Ten neuroplastic genes which individual expression levels were not significantly affected by the UBI were nevertheless dysregulated as the components of the inter- and intra-area co-expression networks. These genes were a neuronal activity-dependent transcription factor *cFos*; *Gap-43* coding for growth-associated protein Gap-43 that regulates axonal growth and neural network formation; brain-derived neurotrophic factor *Bdnf* regulating synaptogenesis; activity-regulated cytoskeletal *Arc* gene implicated in numerous plasticity paradigms; *Egr1* regulating transcription of growth factors, DNA damage and ischaemia genes; *Nfkbia* (I-Kappa-B-Alpha) that inhibits NF-kappa-B/REL complexes regulating activity-dependent inhibitory and excitatory neuronal function; *GluR1* and *Grin2b* coding for the glutamate ionotropic receptor AMPA type subunit 1 and NMDA receptor subunit, respectively, both involved in glutamate signalling and synaptic plasticity; *Homer-1* giving rise to Homer Scaffold Protein 1, a component of glutamate signalling involved in nociceptive plasticity; and *Syt4* (Synaptotagmin 4) playing a role in dendrite formation and synaptic growth and plasticity (Hayashi *et al.*, 2000; Adkins *et al.*, 2006; O'Mahony *et al.*, 2006; Tappe *et al.*, 2006; Vavrek *et al.*, 2006; Larsson and Broman, 2008; Dolan *et al.*, 2011; Grasselli and Strata, 2013; Harris *et al.*, 2016; Epstein and Finkbeiner, 2018).

Changes in the co-expression patterns were likely mediated through the epigenetic and transcriptional mechanisms affected by the UBI, and therefore characterization of the co-regulation phenomenon does not require analysis of protein products of analysed genes. We did not study UBI effects on the levels of neuroplastic proteins. However, the identified increase in the *Tgfb1* mRNA levels corroborated with elevation in the levels of Tgfb1 protein in the spinal lumbar segments after the TBI, and elevation of neurotrophins and inflammatory cytokine expression in the spinal cord after cortical stroke (Sist *et al.*, 2014; Tennant, 2014; Kononenko *et al.*, 2019). It is interesting to examine a role of protein products of three neuroplastic genes affected by the UBI in the brain lesion-induced changes in hindlimb functions.

Clinical studies demonstrated that a large fraction of subjects with stroke and cerebral palsy do not relax their muscles—they are tonically constricted without any voluntary command. This phenomenon is called spastic dystonia and defined as 'stretch- and effort-unrelated sustained involuntary muscle activity following central motor lesions' (Gracies, 2005; Lorentzen *et al.*, 2018). This clinical phenomenon can alter posture at rest thereby contributing to the hemiplegia (Marinelli *et al.*, 2017) and is regarded as a form of efferent muscle hyperactivity (Gracies, 2005; Baude *et al.*, 2019). Spastic dystonia may have a central mechanism which does not depend on afferent input in contrast to spasticity based on exacerbated reflex excitability (Sheean and McGuire, 2009). It was postulated that rhizotomy which abolished sensory input and diminish stretch reflexes would have no effect on spastic dystonia. The example is the absence of effects of dorsal rhizotomy on development of muscle contractures in children with cerebral palsy (Tedroff *et al.*, 2015). A cause of spastic dystonia was experimentally addressed in early studies by Denny-Brown (1966, 1980) who demonstrated that monkeys with lesions of motor cortex display involuntary muscle activity. It persisted following disruption of sensory input to the spinal cord suggesting that a central mechanism but not exaggerated reflexes are involved. Sustained involuntary muscle activity developed in the absence of stretch and voluntary stimulation contributes to body deformities in stroke patients, and thereby it is critical to develop experimental approach for preclinical analysis of spastic dystonia (Gracies, 2005; Marinelli *et al.*, 2017; Pingel *et al.*, 2017; Lorentzen *et al.*, 2018; Baude *et al.*, 2019). The HL-PA that is induced by lesion to the hindlimb sensorimotor cortex and that is not affected by rhizotomy may represent a small animal model for investigation of this phenomenon.

In conclusion, the HL-PA resistance to deafferentation in the spinalized rats may be developed due to the UBI-induced neuroplastic changes in the efferent hindlimb neuromuscular circuits. This finding is concordant with the pathological non-stretch and non-effort-related sustained involuntary muscle activity observed after central motor lesions in clinical situations (Gracies, 2005; Sheean and McGuire, 2009; Tedroff *et al.*, 2015; Marinelli *et al.*, 2017; Lorentzen *et al.*, 2018; Baude *et al.*, 2019). The unusual feature of this phenomenon is its association with the right-side brain lesion. The lateralization of mono- and polysynaptic reflexes (Hultborn and Malmsten, 1983*a*, *b*; Malmsten, 1983) including NWRs and the asymmetry in stretching force support hypothesis on asymmetric organization of the spinal cord. These findings represent a subject for further analyses essential for understanding of motor deficits secondary to stroke and TBI, and basic mechanisms of sensorimotor integration in the spinal cord.

# Supplementary material

Supplementary material is available at *Brain Communications* online.

# Acknowledgements

We are grateful to Mr. Petter Pettersson and Dr. Palmi Thor Thorbergsson for construction of the micromanipulator-controlled force meter device; Dr. Michael Ossipov for discussion and manuscript processing; Dr. Aleh Yahorau for help with figure preparation; and Dr. John Harris, University of Nottingham, Leicestershire, UK for sharing his knowledge on decerebration procedure with us.

# Funding

The study was supported by the Swedish Science Research Council (Grants K2014-62X-12190-19-5 and 2019-01771-3), P.O. Zetterling foundation, Uppsala University, and by grant of the Government of the Russian Federation (14.W03.31.0031).

# Competing interests

The authors report no competing interests.

# References

Adkins DL, Boychuk J, Remple MS, Kleim JA. Motor training induces experience-specific patterns of plasticity across motor cortex and spinal cord. J Appl Physiol 2006; 101: 1776–82.

Alella A. Persistence of asymmetries of cerebral origin in the extremities of animals with cord section. Arch Fisiol 1948; 47: 105–12.

Alvisi E, Serrao M, Conte C, Alfonsi E, Tassorelli C, Prunetti P, et al. Botulinum toxin A modifies nociceptive withdrawal reflex in subacute stroke patients. Brain Behav 2018; 8: e01162.

Andersen OK, Jensen LM, Brennum J, Arendt-Nielsen L. Modulation of the human nociceptive reflex by cyclic movements. Europ J Appl Physiol 1995; 70: 311–21.

Anderson MF, Winterson BJ. Properties of peripherally induced persistent hindlimb flexion in rat: involvement of N-methyl-D-aspartate receptors and capsaicin-sensitive afferents. Brain Res 1995; 678: 140–50.

Aymard C, Katz R, Lafitte C, Lo E, Penicaud A, Pradat-Diehl P, et al. Presynaptic inhibition and homosynaptic depression: a comparison between lower and upper limbs in normal human subjects and patients with hemiplegia. Brain 2000; 123: 1688–702.

Bakalkin G, Iarygin KN, Trushina ED, Titov MI, Smirnov VN. Preferential development of flexion of the left or right hindlimb as a result of treatment with methionine-enkephalin or leucine-enkephalin, respectively. Dokl Akad Nauk SSSR 1980; 252: 762–5.

Bakalkin G, Kobylyansky AG. Opioids induce postural asymmetry in spinal rat: the side of the flexed limb depends upon the type of opioid agonist. Brain Res 1989; 480: 277–89.

Bakalkin G, Kobylyansky AG, Nagornaya LV, Yarygin KN, Titov MI. Met-enkephalin-induced release into the blood of a factor causing postural asymmetry. Peptides 1986; 7: 551–6.

Bakalkin G, Krivosheev OG, Stolyarov GK. Postural asymmetry in rats induced by stress and pain stimuli. Life Sci 1982; 30: 779–83.

Baude M, Nielsen JB, Gracies JM. The neurophysiology of deforming spastic paresis: a revised taxonomy. Ann Phys Rehabil Med 2019; 62: 426–30.

Buisson A, Lesne S, Docagne F, Ali C, Nicole O, MacKenzie ET, et al. Transforming growth factor-beta and ischemic brain injury. Cell Mol Neurobiol 2003; 23: 539–50.

Burkner PC. brms: an R package for Bayesian multilevel models using Stan. Stat Software 2017; 80: 1–28.

Carpenter B, Gelman A, Hoffman MD, Lee D, Goodrich B, Betancourt M, et al. Stan: a probabilistic programming language. Stat Software 2017; 76: 1–31.

Chamberlain TJ, Halick P, Gerard RW. Fixation of experience in the rat spinal cord. J Neurophysiol 1963; 26: 662–73.

Chazov EI, Bakalkin G, Yarigin KN, Trushina ED, Titov MI, Smirnov VN. Enkephalins induce asymmetrical effects on posture in the rat. Experientia 1981; 37: 887–9.

Condliffe EG, Clark DJ, Patten C. Reliability of elbow stretch reflex assessment in chronic post-stroke hemiparesis. Clin Neurophysiol 2005; 116: 1870–8.

Crenna P, Frigo C. Evidence of phase-dependent nociceptive reflexes during locomotion in man. Exp Neurol 1984; 85: 336–45.

de Kovel CGF, Lisgo S, Karlebach G, Ju J, Cheng G, Fisher SE, et al. Left-right asymmetry of maturation rates in human embryonic neural development. Biol Psychiatry 2017; 82: 204–12.

Delwaide PJ, Oliver E. Short-latency autogenic inhibition (IB inhibition) in human spasticity. J Neurol Neurosurg Psychiatry 1988; 51: 1546–50.

Denny-Brown D. The cerebral control of movement. Liverpool: Liverpool University Press; 1966. p. 210–7.

Denny-Brown D. Preface: historical aspects of the relation of spasticity to movement. In: RG Feldman, RR Young, WP Koella, editors. Spasticity: disordered motor control. Chicago: Yearbook Medical; 1980. p. 1–16.

Dietz V, Grillner S, Trepp A, Hubli M, Bolliger M. Changes in spinal reflex and locomotor activity after a complete spinal cord injury: a common mechanism? Brain 2009; 132: 2196–205.

DiGiorgio AM. Persistence of postural and motor asymmetries of cerebellar origin in spinal animals: I, II, III. Arch Fisiol 1929; 27: 518–80.

DiGiorgio AM. Influences of the cerebellum-neocerebellum on the postural tone of the limbs and cerebellar somatotopy in the rhomboencephalic animal. Arch Fisiol 1942; 42: 25–79.

Dobrin R, Zhu J, Molony C, Argman C, Parrish ML, Carlson S, et al. Multi-tissue coexpression networks reveal unexpected subnetworks associated with disease. Genome Biol 2009; 10: R55.

Dolan S, Hastie P, Crossan C, Nolan AM. Co-induction of cyclooxygenase-2 [correction of cyclooxyenase-2] and early growth response gene (Egr-1) in spinal cord in a clinical model of persistent inflammation and hyperalgesia. Mol Pain 2011; 7: 91.

Duysens J, Tax AA, Trippel M, Dietz V. Phase-dependent reversal of reflexly induced movements during human gait. Exp Brain Res 1992; 90: 404–14.

Duysens J, Trippel M, Horstmann GA, Dietz V. Gating and reversal of reflexes in ankle muscles during human walking. Exp Brain Res 1990; 82: 351–8.

Emborg J, Spaich EG, Andersen OK. Withdrawal reflexes examined during human gait by ground reaction forces: site and gait phase dependency. Med Biol Eng Comput 2009; 47: 29–39.

Epstein I, Finkbeiner S. The Arc of cognition: signaling cascades regulating Arc and implications for cognitive function and disease. Semin Cell Dev Biol 2018; 77: 63–72.

Eriksson J, Olausson B, Jankowska E. Antispastic effects of L-dopa. Exp Brain Res 1996; 111: 296–304.

Feldman AG, Levin MF. Spatial control of reflexes, posture and movement in normal conditions and after neurological lesions. J Hum Kinet 2016; 52: 21–34.

Fernandes CA, Coelho DB, Martinelli AR, Teixeira LA. Cerebral hemisphere specialization for quiet and perturbed body balance control: evidence from unilateral stroke. Hum Mov Sci 2018; 57: 374–87.

Frigon A, Barriere G, Leblond H, Rossignol S. Asymmetric changes in cutaneous reflexes after a partial spinal lesion and retention following spinalization during locomotion in the cat. J Neurophysiol 2009; 102: 2667–80.

Frigon A, Johnson MD, Heckman CJ. Altered activation patterns by triceps surae stretch reflex pathways in acute and chronic spinal cord injury. J Neurophysiol 2011; 106: 1669–78.

Fuchigami T, Kakinohana O, Hefferan MP, Lukacova N, Marsala S, Platoshyn O, et al. Potent suppression of stretch reflex activity after systemic or spinal delivery of tizanidine in rats with spinal ischemia-induced chronic spastic paraplegia. Neuroscience 2011; 194: 160–9.

Gelman A. Prior choice recommendations. In: GitHub, editor. Stan-dev/stan; 2019.

Gervasio S, Laursen CB, Andersen OK, Hennings K, Spaich EG. A novel stimulation paradigm to limit the habituation of the nociceptive withdrawal reflex. IEEE Trans Neural Syst Rehabil Eng 2018; 26: 1100–7.

Gossard JP, Delivet-Mongrain H, Martinez M, Kundu A, Escalona M, Rossignol S. Plastic changes in lumbar locomotor networks after a partial spinal cord injury in cats. J Neurosci 2015; 35: 9446–55.

Gracies JM. Pathophysiology of spastic paresis. I: Paresis and soft tissue changes. Muscle Nerve 2005; 31: 535–51.

Grasselli G, Strata P. Structural plasticity of climbing fibers and the growth-associated protein GAP-43. Front Neural Circuits 2013; 7: 25.

Grau JW. Learning from the spinal cord: how the study of spinal cord plasticity informs our view of learning. Neurobiol Learn Memory 2014; 108: 155–71.

Harris KP, Zhang YV, Piccioli ZD, Perrimon N, Littleton JT. The postsynaptic t-SNARE Syntaxin 4 controls traffic of Neuroligin 1 and Synaptotagmin 4 to regulate retrograde signaling. eLife 2016; 5: e13881.

Hayashi M, Ueyama T, Nemoto K, Tamaki T, Senba E. Sequential mRNA expression for immediate early genes, cytokines, and neurotrophins in spinal cord injury. J Neurotrauma 2000; 17: 203–18.

Hubli M, Bolliger M, Limacher E, Luft AR, Dietz V. Spinal neuronal dysfunction after stroke. Exp Neurol 2012; 234: 153–60.

Hultborn H, Malmsten J. Changes in segmental reflexes following chronic spinal cord hemisection in the cat. I. Increased monosynaptic and polysynaptic ventral root discharges. Acta Physiol Scand 1983a; 119: 405–22.

Hultborn H, Malmsten J. Changes in segmental reflexes following chronic spinal cord hemisection in the cat. II. Conditioned monosynaptic test reflexes. Acta Physiol Scand 1983b; 119: 423–33.

Jankowska E. Interneuronal relay in spinal pathways from proprioceptors. Prog Neurobiol 1992; 38: 335–78.

Jones TA. Motor compensation and its effects on neural reorganization after stroke. Nat Rev Neurosci 2017; 18: 267–80.

Joynes RL, Janjua K, Grau JW. Instrumental learning within the spinal cord: VI. The NMDA receptor antagonist, AP5, disrupts the acquisition and maintenance of an acquired flexion response. Behav Brain Res 2004; 154: 431–8.

Kawakami R, Shinohara Y, Kato Y, Sugiyama H, Shigemoto R, Ito I. Asymmetrical allocation of NMDA receptor epsilon2 subunits in hippocampal circuitry. Science 2003; 300: 990–4.

Kerzoncuf M, Bensoussan L, Delarque A, Durand J, Viton JM, Rossi-Durand C. Plastic changes in spinal synaptic transmission following botulinum toxin A in patients with post-stroke spasticity. J Rehabil Med 2015; 47: 910–6.

Klement'ev BI, Molokoedov AS, Bushuev VN, Danilovskii MA, Sepetov NF. Isolation of the postural asymmetry factor following right hemisection of the spinal cord. Dokl Akad Nauk SSSR 1986; 291: 737–41.

Knebel D, Rillich J, Ayali A, Pfluger HJ, Rigosi E. Ex vivo recordings reveal desert locust forelimb control is asymmetric. Curr Biol 2018; 28: R1290–1.

Kohl MM, Shipton OA, Deacon RM, Rawlins JN, Deisseroth K, Paulsen O. Hemisphere-specific optogenetic stimulation reveals left-right asymmetry of hippocampal plasticity. Nat Neurosci 2011; 14: 1413–5.

Kononenko O, Galatenko V, Andersson M, Bazov I, Watanabe H, Zhou XW, et al. Intra- and interregional coregulation of opioid genes: broken symmetry in spinal circuits. FASEB J 2017; 31: 1953–63.

Kononenko O, Mityakina I, Galatenko V, Watanabe H, Bazov I, Gerashchenko A, et al. Differential effects of left and right neuropathy on opioid gene expression in lumbar spinal cord. Brain Res 2018; 1695: 78–83.

Kononenko O, Watanabe H, Stalhandske L, Zarelius A, Clausen F, Yakovleva T, et al. Focal traumatic brain injury induces neuroplastic molecular response in lumbar spinal cord. Restor Neurol Neurosci 2019; 37: 87–96.

Larsson M, Broman J. Translocation of GluR1-containing AMPA receptors to a spinal nociceptive synapse during acute noxious stimulation. J Neurosci 2008; 28: 7084–90.

Lavrov I, Gerasimenko Y, Burdick J, Zhong H, Roy RR, Edgerton VR. Integrating multiple sensory systems to modulate neural networks controlling posture. J Neurophysiol 2015; 114: 3306–14.

Long Q, Argmann C, Houten SM, Huang T, Peng S, Zhao Y, et al.; The GTEx Consortium. Inter-tissue coexpression network analysis reveals DPP4 as an important gene in heart to blood communication. Genome Med 2016; 8: 15.

Lorentzen J, Pradines M, Gracies JM, Bo Nielsen J. On Denny-Brown's 'spastic dystonia'—what is it and what causes it? Clin Neurophysiol 2018; 129: 89–94.

Lukoyanov N, Carvalho L, Watanabe H, Zhang M, Sarkisyan D, Kononenko O, et al. Contralesional hindlimb motor response induced by unilateral brain injury: evidence for extra spinal mechanism. J Neurotrauma 2018; 35: A-2–A-201; PS2.04.57.

Malmsten J. Time course of segmental reflex changes after chronic spinal cord hemisection in the rat. Acta Physiol Scand 1983; 119: 435–43.

Marinelli L, Curra A, Trompetto C, Capello E, Serrati C, Fattapposta F, et al. Spasticity and spastic dystonia: the two faces of velocity-dependent hypertonia. J Electromyogr Kinesiol 2017; 37: 84–9.

Marque P, Simonetta-Moreau M, Maupas E, Roques CF. Facilitation of transmission in heteronymous group II pathways in spastic hemiplegic patients. J Neurol Neurosurg Psychiatry 2001; 70: 36–42.

McElreath R. Statistical rethinking: a bayesian course with examples in R and Stan. Chapman and Hall/CRC; 2020.

Miller JF, Paul KD, Lee RH, Rymer WZ, Heckman CJ. Restoration of extensor excitability in the acute spinal cat by the 5-HT2 agonist DOI. J Neurophysiol 1996; 75: 620–8.

Murphy TH, Corbett D. Plasticity during stroke recovery: from synapse to behaviour. Nat Rev Neurosci 2009; 10: 861–72.

Musienko PE, Zelenin PV, Orlovsky GN, Deliagina TG. Facilitation of postural limb reflexes with epidural stimulation in spinal rabbits. J Neurophysiol 2010; 103: 1080–92.

Nathan PW, Smith MC, Deacon P. The corticospinal tracts in man. Course and location of fibres at different segmental levels. Brain 1990; 113: 303–24.

O'Mahony A, Raber J, Montano M, Foehr E, Han V, Lu S-M, et al. NF-kappaB/Rel regulates inhibitory and excitatory neuronal function and synaptic plasticity. Mol Cell Biol 2006; 26: 7283–98.

Ocklenburg S, Schmitz J, Moinfar Z, Moser D, Klose R, Lor S, et al. Epigenetic regulation of lateralized fetal spinal gene expression underlies hemispheric asymmetries. eLife 2017; 6:

Patterson MM. Spinal fixation: long-term alterations in spinal reflex excitability with altered or sustained sensory inputs. In: MM Patterson, JW Grau, editors. Spinal cord plasticity. Boston: Springer; 2001. p. 77–99.

Pearlson GD, Robinson RG. Suction lesions of the frontal cerebral cortex in the rat induce asymmetrical behavioral and catecholaminergic responses. Brain Res 1981; 218: 233–42.

Perennou DA, Mazibrada G, Chauvineau V, Greenwood R, Rothwell J, Gresty MA, et al. Lateropulsion, pushing and verticality perception in hemisphere stroke: a causal relationship? Brain 2008; 131: 2401–13.

Pin-Barre C, Laurin J. Physical exercise as a diagnostic, rehabilitation, and preventive tool: influence on neuroplasticity and motor recovery after stroke. Neural Plasticity 2015; 2015: 1–12.

Pingel J, Bartels EM, Nielsen JB. New perspectives on the development of muscle contractures following central motor lesions. J Physiol 2017; 595: 1027–38.

R Core Team. R: a language and environment for statistical computing. In: Computing RFfS, editor. 2.6.2 (2008-02-08) ed. Vienna, Austria; 2018.

Robinson RG. Differential behavioral and biochemical effects of right and left hemispheric cerebral infarction in the rat. Science 1979; 205: 707–10.

Roelofs JMB, van Heugten K, de Kam D, Weerdesteyn V, Geurts A. Relationships between affected-leg motor impairment, postural asymmetry, and impaired body sway control after unilateral supratentorial stroke. Neurorehabil Neural Repair 2018; 32: 953–60.

Rossi A, Decchi B. Flexibility of lower limb reflex responses to painful cutaneous stimulation in standing humans: evidence of load-dependent modulation. J Physiol 1994; 481: 521–32.

Rossignol S, Frigon A. Recovery of locomotion after spinal cord injury: some facts and mechanisms. Annu Rev Neurosci 2011; 34: 413–40.

Rousseaux M, Honore J, Saj A. Body representations and brain damage. Neurophysiol Clin 2014; 44: 59–67.

Rueterbories J, Spaich EG, Andersen OK. Characterization of gait pattern by 3D angular accelerations in hemiparetic and healthy gait. Gait Posture 2013; 37: 183–9.

Sainburg RL. Convergent models of handedness and brain lateralization. Front Psychol 2014; 5: 1092.

Sainburg RL, Maenza C, Winstein C, Good D. Motor lateralization provides a foundation for predicting and treating non-paretic arm motor deficits in stroke. Adv Exp Med Biol 2016; 957: 257–72.

Sandrini G, Serrao M, Rossi P, Romaniello A, Cruccu G, Willer JC. The lower limb flexion reflex in humans. Prog Neurobiol 2005; 77: 353–95.

Santibanez JF, Quintanilla M, Bernabeu C. TGF-beta/TGF-beta receptor system and its role in physiological and pathological conditions. Clin Sci 2011; 121: 233–51.

Schouenborg J. Modular organisation and spinal somatosensory imprinting. Brain Res Brain Res Rev 2002; 40: 80–91.

Schouenborg J, Holmberg H, Weng HR. Functional organization of the nociceptive withdrawal reflexes. II. Changes of excitability and receptive fields after spinalization in the rat. Exp Brain Res 1992; 90: 469–78.

Searle SR, Speed FM, Milliken GA. Population marginal means in the linear model: an alternative to least squares means. Am Stat 1980; 34: 216–21.

Serrao M, Ranavolo A, Andersen OK, Don R, Draicchio F, Conte C, et al. Reorganization of multi-muscle and joint withdrawal reflex during arm movements in post-stroke hemiparetic patients. Clin Neurophysiol 2012; 123: 527–40.

Sheean G, McGuire JR. Spastic hypertonia and movement disorders: pathophysiology, clinical presentation, and quantification. PM R 2009; 1: 827–33.

Sist B, Fouad K, Winship IR. Plasticity beyond peri-infarct cortex: spinal up regulation of structural plasticity, neurotrophins, and inflammatory cytokines during recovery from cortical stroke. Exp Neurol 2014; 252: 47–56.

Spaich EG, Arendt-Nielsen L, Andersen OK. Modulation of lower limb withdrawal reflexes during gait: a topographical study. J Neurophysiol 2004; 91: 258–66.

Spaich EG, Hinge HH, Arendt-Nielsen L, Andersen OK. Modulation of the withdrawal reflex during hemiplegic gait: effect of stimulation site and gait phase. Clin Neurophysiol 2006; 117: 2482–95.

Spaich EG, Svaneborg N, Jorgensen HR, Andersen OK. Rehabilitation of the hemiparetic gait by nociceptive withdrawal reflex-based functional electrical therapy: a randomized, single-blinded study. J Neuroeng Rehabil 2014; 11: 81.

Spinazzola L, Cubelli R, Della Sala S. Impairments of trunk movements following left or right hemisphere lesions: dissociation between apraxic errors and postural instability. Brain 2003; 126: 2656–66.

Stancher G, Sovrano VA, Vallortigara G. Motor asymmetries in fishes, amphibians, and reptiles. Prog Brain Res 2018; 238: 33–56.

Straka H, Dieringer N. Spinal plasticity after hemilabyrinthectomy and its relation to postural recovery in the frog. J Neurophysiol 1995; 73: 1617–31.

Tan AM, Chakrabarty S, Kimura H, Martin JH. Selective corticospinal tract injury in the rat induces primary afferent fiber sprouting in the spinal cord and hyperreflexia. J Neurosci 2012; 32: 12896–908.

Tandon S, Kambi N, Jain N. Overlapping representations of the neck and whiskers in the rat motor cortex revealed by mapping at different anaesthetic depths. Eur J Neurosci 2007; 27: 228–37.

Tappe A, Klugmann M, Luo C, Hirlinger D, Agarwal N, Benrath J, et al. Synaptic scaffolding protein Homer1a protects against chronic inflammatory pain. Nat Med 2006; 12: 677–81.

Tasseel-Ponche S, Yelnik AP, Bonan IV. Motor strategies of postural control after hemispheric stroke. Neurophysiol Clin 2015; 45: 327–33.

Tedroff K, Lowing K, Astrom E. A prospective cohort study investigating gross motor function, pain, and health-related quality of life 17 years after selective dorsal rhizotomy in cerebral palsy. Dev Med Child Neurol 2015; 57: 484–90.

Tennant KA. Thinking outside the brain: structural plasticity in the spinal cord promotes recovery from cortical stroke. Exp Neurol 2014; 254: 195–9.

Thilmann AF, Fellows SJ, Ross HF. Biomechanical changes at the ankle joint after stroke. J Neurol Neurosurg Psychiatry 1991; 54: 134–9.

Valero-Cabre A, Fores J, Navarro X. Reorganization of reflex responses mediated by different afferent sensory fibers after spinal cord transection. J Neurophysiol 2004; 91: 2838–48.

Varlinskaia EI, Rogachii MG, Klement'ev BI, Vartanian GA. Dynamics of the activity of the postural asymmetry factor after unilateral damage to the motor area of the cortex. Biull Eksp Biol Med 1984; 98: 281–3.

Vartanyan GA, Klementiev BI. Chemical symmetry and asymmetry of the brain. Leningrad: Nauka; 1991.

Vavrek R, Girgis J, Tetzlaff W, Hiebert GW, Fouad K. BDNF promotes connections of corticospinal neurons onto spared descending interneurons in spinal cord injured rats. Brain 2006; 129: 1534–45.

Weng HR, Schouenborg J. Cutaneous inhibitory receptive fields of withdrawal reflexes in the decerebrate spinal rat. J Physiol 1996; 493: 253–65.

Wilson L, Stewart W, Dams-O'Connor K, Diaz-Arrastia R, Horton L, Menon DK, et al. The chronic and evolving neurological consequences of traumatic brain injury. Lancet Neurol 2017; 16: 813–25.

Wilson LR, Gandevia SC, Inglis JT, Gracies J, Burke D. Muscle spindle activity in the affected upper limb after a unilateral stroke. Brain 1999; 122: 2079–88.

Wolpaw JR. Harnessing neuroplasticity for clinical applications. Brain 2012; 135: e215.

Won S, Incontro S, Nicoll RA, Roche KW. PSD-95 stabilizes NMDA receptors by inducing the degradation of STEP61. Proc Natl Acad Sci USA 2016; 113: E4736–44.

Woytowicz EJ, Westlake KP, Whitall J, Sainburg RL. Handedness results from complementary hemispheric dominance, not global hemispheric dominance: evidence from mechanically coupled bilateral movements. J Neurophysiol 2018; 120: 729–40.

Wu Y, Kawakami R, Shinohara Y, Fukaya M, Sakimura K, Mishina M, et al. Target-cell-specific left-right asymmetry of NMDA receptor content in schaffer collateral synapses in epsilon1/NR2A knock-out mice. J Neurosci 2005; 25: 9213–26.

You HJ, Morch CD, Arendt-Nielsen L. Electrophysiological characterization of facilitated spinal withdrawal reflex to repetitive electrical stimuli and its modulation by central glutamate receptor in spinal anesthetized rats. Brain Res 2004; 1009: 110–9.

Zhou HH, Jin TT, Qin B, Turndorf H. Suppression of spinal cord motoneuron excitability correlates with surgical immobility during isoflurane anesthesia. Anesthesiology 1998; 88: 955–61.